Special Feature: Power Electronics for Hybrid Vehicles

Research Report

High-voltage Power Line Communication System for Hybrid Vehicle

Masaki Takanashi, Tomohisa Harada, Atsuhiro Takahashi, Hiroya Tanaka, Hiroaki Hayashi and Yoshiyuki Hattori

Report received on Feb. 27, 2017

ABSTRACT Recently, hybrid vehicles (HVs) and electric vehicles (EVs) have become widespread. These vehicles incorporate a large number of electronic devices. In HVs and EVs, a high-voltage (200 V) battery is employed. In the current HVs, the battery supplies power to the Power Control Unit (PCU) for driving a motor, generator and air conditioner compressor. It is expected that such kinds of power electronic devices will increase in number in the future. In this paper, we propose a high-voltage PLC and present the development of a high-voltage PLC system that can simultaneously control multiple power electronic devices in real time.

First, in a system simulating the structure of a commercially available HV, the results of transmission characteristics and electromagnetic noise characteristics that are superimposed on the high-voltage power line are shown. From these results, the optimum carrier frequency as a PLC is revealed. Then, the bit error rate (BER) performance under the above noise environment is clarified by computer simulations. In consideration of the above, specifications of the PLC system of the HV are developed. Finally, we construct a prototype of the high-voltage PLC system and demonstrate that the system can simultaneously control the rotational speed of two motors.

KEYWORDS Hybrid Vehicle, High-voltage Power Line, Electric Devices, Motor Rotation Control, Prototype

1. Introduction

With the recent surging popularity of hybrid vehicles (HVs) and electric vehicles (EVs), the number of electronic devices such as electronic control units (ECUs), sensors, and actuators that have been incorporated into such vehicles has grown as well. However, the increasing number of such devices is also raising concerns due to the number of communication lines and connectors that they require, not only because vehicle weight increases but also due to concerns such as finding sufficient space for the necessary wiring. One attractive method of solving such issues involves the use of power line communication (PLC) in such vehicles.

While numerous previous studies have been performed on vehicle PLC uses,[1-7] most have focused on low-voltage (12 V) power supply lines (**Fig. 1**) in which current flows into the electronic device through a positive line and returns via the vehicle body metal. This method, however, can result in issues such as electromagnetic interference (EMI) in other vehicles and external noise resistance. In contrast to conventional vehicle low-voltage systems, HVs are equipped with a high-voltage (200 V) battery (**Fig. 2**) that supplies current to a power control unit (PCU) where it is then subdivided to drive electric motors, the generator, and the air conditioner compressor.

Since it is anticipated that future HVs and EVs will use this high voltage to power other electronic devices such as blowers, and both the oil and water pumps, and since this current will be carried over two parallel (positive (P) and negative (N)) wires bound within a shielded sheath, we propose a high-voltage capable PLC that will significantly reduce 12 V power supply line noise issues. In this paper, we report on the development of our proposed high-voltage line PLC (HV-PLC) system, which can simultaneously control power to multiple electronic devices in real time, and demonstrate its operation.

This paper begins with an evaluation of the transmission characteristics of the power line so as to ascertain the optimum carrier frequency of the PLC, after which we look at the noise characteristics that are overlaid on the line of a commercially available HV. Computer simulations are conducted to disclose

the bit error rate (BER) performance under the clarified noise environment.

We then determine the system specifications of a dedicated communication device that will be used in the prototype of our proposed high-voltage line PLC system and demonstrate how it can be used to simultaneously control the rotational speed of two motors.

In this paper, firstly to reveal the optimum carrier frequency of the PLC, we evaluate the transmission characteristics of the power supply line and the noise characteristics that are superimposed on the line of the commercially available HV. Also, the bit error rate (BER) performance under the noise environment is revealed by computer simulations.

Next, to construct dedicated communication device, we clarify the system specifications. Finally, a high-voltage line PLC system using the communication device is prototyped. The high-voltage line PLC system that can simultaneously control the rotational speed of two motors is demonstrated.

2. Requirements for High-voltage PLC System

In the proposed PLC, we consider to connect power electronic devices such as water pump, blower, and air-conditioner along with the main line connecting between the PCU and the high-voltage battery as shown in Fig. 2. Under this configuration, communication device mounted in the PCU becomes the mother computer and controls the rotational speed of motors mounted in the electronic devices via the high-voltage line.

Then, the data volume to control each motor requires 70 bytes. In addition, to ensure at least 99% reliability of the transmission of control commands to each motor, it is necessary for the BER to be less than 1×10^{-5}. The bits for error correction and synchronization are added to the user data of 70 bytes, and so the length of the transmission packet becomes 140 bytes.

The transmission period and delay of the data must be less than 8 ms, because these motors must be immediately responsive to the commands of the

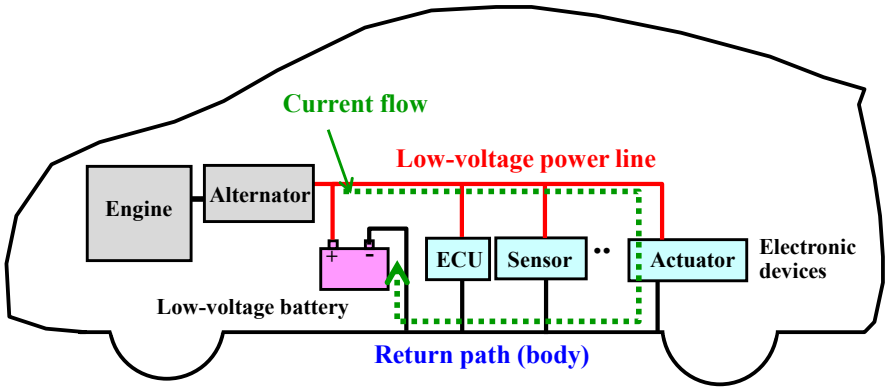

Fig. 1 Current flow of high-voltage power line in conventional vehicle.

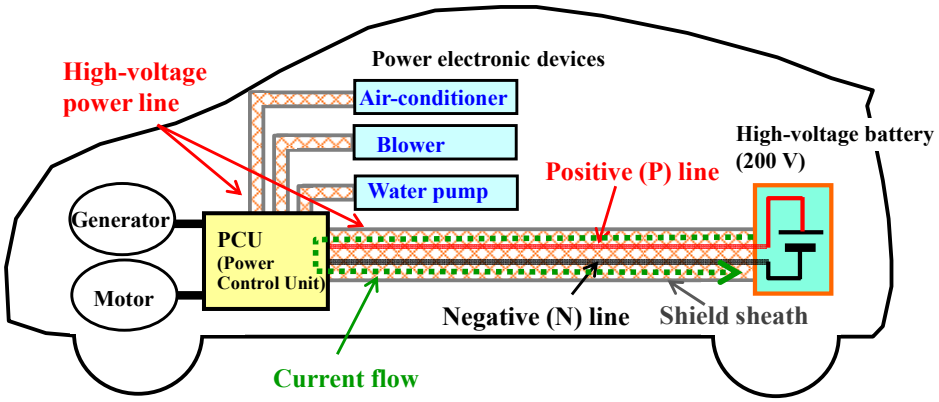

Fig. 2 Current flow of high-voltage power line in hybrid vehicle.

mother computer. To satisfy the requirement, a transmission rate of 350 kbps for each device is necessary. Because we assume that the maximum number of devices connected to the high-voltage line is five at most, the transmission speed becomes 1.75 Mbps in total. Considering the margin, we set 2 Mbps as the target transmission speed for our high-voltage PLC.

3. Transmission and Electromagnetic Noise Characteristics of the HV

In this section, the transmission characteristics of the high-voltage power line and the noise characteristics that are superimposed on the power line are evaluated in the system simulating the structure of a commercially available HV. From the results, the optimum carrier frequency of the PLC is revealed.

3. 1 Transmission Characteristics

The transmission characteristics between the PCU and motor 1 are measured by a vector network analyzer (VNA) (Agilent E5071C) in the system as shown in **Fig. 3**. Through this paper, we assume the network topology where an electronic device is connected to the PCU and communication each other. The length of the high-voltage power line between them is 4 m. To protect the devices from the high voltage, we insert capacitors and a transformer between the power line and the VNA.

The measurement results of the transmission characteristics are shown in **Fig. 4**. We can see that the transmission characteristics are stable between −20 dB to −30 dB in the frequency range of a few MHz to 30 MHz, although these characteristics are degraded under 1 MHz. The deterioration at the frequency less than 1 MHz is the effect of the smoothing capacitor mounted in the PCU as shown in Fig. 3.

3. 2 Electromagnetic Noise over the HV-PLC Line

Electromagnetic noise is imposed over the transmission channel while operating the DC-DC converter and inverter in the PCU. We therefore observed DC-DC converter noise, which has the largest amplitude in the HV system. Then, we connect an analog-to-digital converter to the connecting point between PCU and the PN line. In addition, we also connect a 50 Ω termination to the connecting point between the electronic device and the PN line. These are connected to the same points to which the VNA was connected as shown in Fig. 3, respectively.

Figure 5 shows the time-domain noise waveform. We employed the analog-to-digital converter (ADC) having a sampling resolution of 14 bits and a rate of 80M samples/s. From the observed data, we see that the characteristic of the noise is not impulsive but continuous. We analyze the frequency domain noise characteristics by applying FFT to the observed time domain noise in Fig. 5. Then, we applied a 256-point FFT, whose time span corresponds to 3.2 μs, to some of the blocks in the time domain. We obtained an averaged frequency domain noise from the blocks. **Figure 6** shows the noise characteristics. We also show the thermal noise of the ADC when the DC-DC converter is off as a comparison, which is equivalent to the thermal noise. From these results, we can see that the noise having a power greater than −45 dBm/kHz exists at less than 1 MHz. MOSFET is

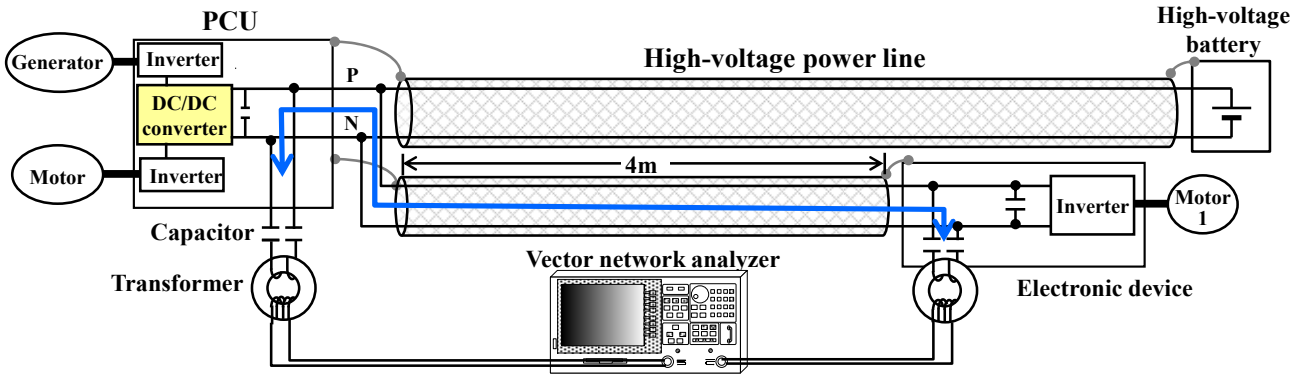

Fig. 3 Measurement of the transmission channel using a vector network analyzer.

deployed in the PCU. The MOSFET generates wideband noise by its switching and the noise is injected into the high-voltage PLC network. This peak noise seems to be occurred by a resonant frequency which is caused by various inductance, capacitance and resistance components which configure the network. This frequency is around 400 kHz. Meanwhile, we can also see that the noise at more than 10 MHz is 40 dB less than the peak noise, which, however, cannot be ignored against the thermal noise in the ADC.

From Figs. 4 and 6, we clarified that we can obtain large signal-to-noise ratio (SNR) margin by employing a carrier frequency that is more than 10 MHz for our HV-PLC.

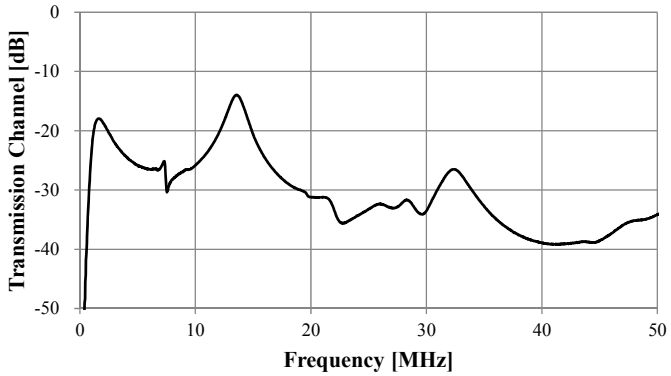

Fig. 4 Transmission channel performance of the PLC.

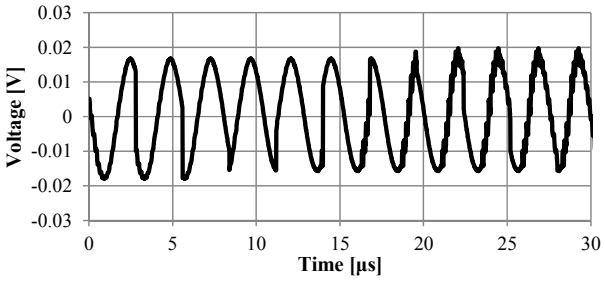

Fig. 5 Time domain noise of the DC-DC converter.

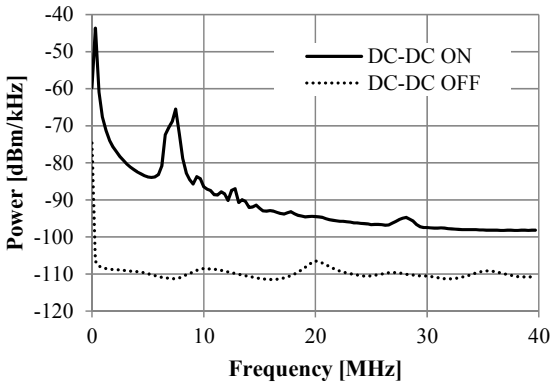

Fig. 6 Frequency domain noise of the DC-DC converter.

In this PLC, we focus on narrow-band single-carrier transmission to achieve a low-cost communication system, which aims at 2 Mbps as the transmission rate, as discussed in Sec. 2. We evaluate the time domain noise characteristic of the communication bandwidth in the case that the following raised cosine filter is employed. We set the carrier frequency f as 15 MHz, which is where good SNR performance is expected. The half bandwidth and roll-off factor β are 2.5 MHz and 0.5, respectively.

$$H(f)=\begin{cases} T & 0 \le |f| < \frac{1-\beta}{2T} \\ \frac{T}{2}\{1+\cos[\frac{\pi T}{\beta}(|f|-\frac{1-\beta}{2T})]\} & \frac{1-\beta}{2T} \le |f| < \frac{1+\beta}{2T} \\ 0 & \frac{1+\beta}{2T} \le |f| \end{cases} \quad (1)$$

Figure 7 shows the band-limited time domain noise of the DC-DC converter and the autocorrelation, respectively. From this figure, we can see the impulsive characteristic of the noise even though the majority of the noise is suppressed by the filter. In addition, we can see that its interval is approximately 6 μs because the correlation value is large approximately every 6 μs.

We show the probability distribution function (PDF) of the amplitude of the band-limited DC-DC converter noise in **Fig. 8**.

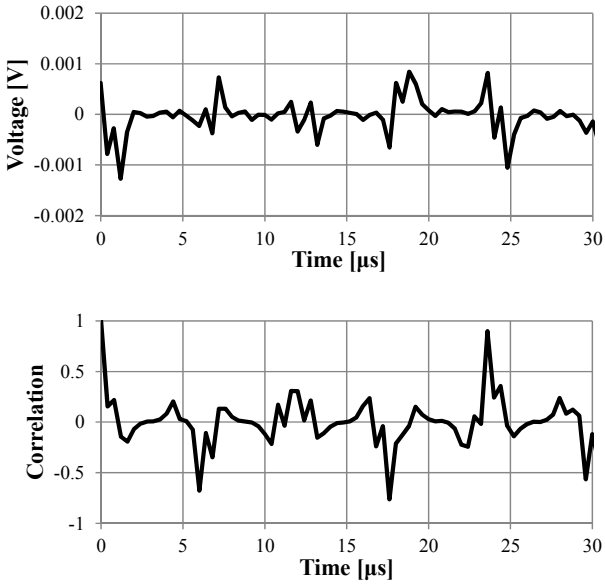

Fig. 7 Voltage and correlation of the band-limited time domain noise of the DC-DC converter.

As a comparison, we also show the PDF of Gaussian noise, whose variance corresponds to that of the DC-DC converter.

We can see that the PDF curve of the DC-DC noise is quite different from that of the Gaussian curve. From the above results, we can say that the band-limited DC-DC converter noise has a periodical and impulsive characteristic that differs from that of thermal Gaussian noise.

4. BER Performance of HV-PLC

In this section, we evaluate the BER performance of the HV-PLC under the DC-DC converter noise environment. The performance was evaluated through computer simulations. We show the simulation parameters in **Table 1**. For these simulations, we employed the filter described in the previous section as a transmitting and receiving filter. We also employed convolutional coding (CC) as forward error correction (FEC). We set the code rate R and the constraint length K at 1/2 and 7, respectively. In this paper, we assumed that synchronization and channel estimation could be ideally done.

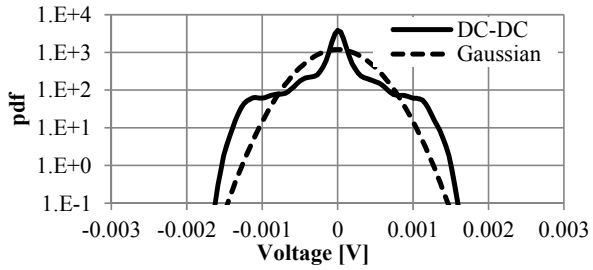

Fig. 8 PDF of the band-limited time domain noise of the DC-DC.

Table 1 Simulation parameters.

Item	Value
Modulation	QPSK
Packet length	120 bytes
Carrier frequency	15 MHz
Receiving filter	Raised-cosine filter (1/T = 2.5 MHz, roll off = 0.5)
Forward error correction	Convolutional code (R = 1/2, K = 7)

We show the simulation results in **Fig. 9**. The solid lines show the performance with the DC-DC converter noise, and the broken lines show the performance with ideal Gaussian noise, whose variance corresponds to that of the DC-DC converter.

From the results, BER $< 1 \times 10^{-5}$ can be achieved with transmission power −27 dBm in the case of uncoded transmission, and with −35 dBm in the case of coded transmission. Therefore, we can obtain a performance gain of 7 dB by employing the CC. Reference (8) showed that the BER performance of the CC was significantly deteriorated under an impulse noise environment and so they proposed an improved decoding method. However, we could not observe such performance under our HV-PLC environment. In Ref. (8), class-A noise, where extremely large noise can be generated, was assumed. On the other hand, in our environment, extremely large noise cannot be generated, because the amplitude of the impulse noise cannot exceed the power supply amplitude, which is 200 V. From these results, we clarified that we could achieve BER performance improvement with the usual coding and decoding framework of the CC in this HV-PLC.

5. Specifications of the HV-PLC Prototype

Based on the requirements set in Sec. 2 and the electromagnetic noise characteristics of the HV, as well as the communication characteristics of the PLC shown in Secs. 3 and 4, we discuss the specifications of the communication device used in this PLC.

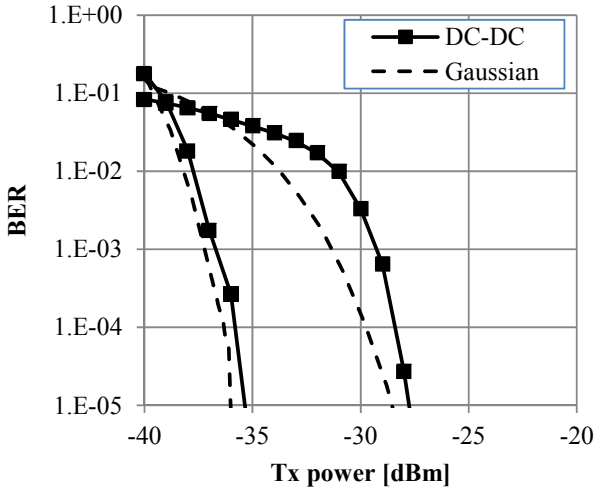

Fig. 9 BER performance under the DC-DC converter noise.

5. 1 Multiple Access Method

Since up to five electronic devices are controlled and the configuration of the communication device is simple, we employ Time Division Multiple Access Time Division Duplex (TDMA-TDD) as the communication control method.

5. 2 Transmission Packet Length

Transmission data eventually reach each power electronic device through three communication channels: (i) from the mother microcomputer to the mother PLC transmitter, (ii) from the mother PLC transmitter to the PLC receiver at the device, and (iii) from the PLC receiver at the device to the microcomputer at the device. In steps (i) and (iii), only a few pieces of information are added to the user information. On the other hand, we employ several communication control bytes for synchronization between transceivers, error detection, and packet detection. Then, we set the size of the transmission packet to 163 bytes by adding 93 control bytes to the user information bytes.

5. 3 Data Transmission Rate

We set the transmission rate to 2 Mbps, as described in Sec. 2. In steps (i) and (iii), we employ a serial peripheral interface (SPI), whose transmission rate is 10 Mbps.

5. 4 Carrier Frequency

Because we could obtain large SNR margin at the carrier frequency from 10 MHz to 30 MHz, we employ a carrier frequency of 16 MHz. This is also a reason that we can easily generate a carrier frequency because the frequency is an exponential of 2 in a transmission rate.

5. 5 Modulation Scheme and Forward Error Correction

Based on the results described in Sec. 4, as the modulation scheme, we employ differential quadrate phase shift keying (DQPSK), which does not need channel estimation, and employ the CC (R = 1/2, K = 7) as the FEC. The other advantage is that we can exploit the abundant IP core.

We show the specifications for the prototype from the above characteristics in **Table 2**.

6. Prototype of the HV-PLC Transceiver

We developed the HV-PLC prototype to accomplish real-time control of multiple power electronic devices. **Figure 10** shows the functional block diagram. The prototype is composed of the FPGA board, AD/DA board and high-voltage line I/F. The FPGA board comprises digital circuits for communication control, TDMA-TDD timing control, FEC, and modulation. The 16 MHz signal is output from the AD, and input to the DA. The high-voltage line I/F employs a transmitting and receiving switch controlled by the TDMA-TDD timing circuit, a band-pass filter (BPF) that eliminates the noise except for the transmission band, and a transformer and a protection diode that protect the boards from the high voltage. We show a photo of the prototype in **Fig. 11**. Although the current prototype is relatively large, we can develop a smaller communication device by employing an integrated circuit (IC). Then, we will be able to use the IC to power the electronic device.

7. Real-time Control of Multiple Motors by the High-voltage PLC

Using the prototype communication device shown in Fig. 11, a PLC system that has the ability to realize real-time control of the speed of two electronic devices (blower, water pump) is developed.

Table 2 Specifications of high-voltage PLC system.

Item	Value
Carrier frequency	16 MHz
Modulation scheme	DQPSK
Data transmission rate	2 Mbps
Forward error correction	Convolutional code
Packet length	163 bytes
User data length	70 bytes
Multiple access method	TDMA-TDD
Packet transmission period	8 ms
Number of slots	5

Figures 12 and **13** show the configuration and photo of the system, respectively.

In this system, when the control PC sends a command instruction setting the rotational speed of the blower and the water pump to the mother microcomputer, the rotational speed command is transferred to the corresponding device. At the same time, the rotational number of the current device gives feedback to the control PC and then is displayed on the PC.

An example of the transmission signal of the mother communication device and the motor communication device is shown in **Fig. 14**. The blower (device 1) and the water pump (device 2) are assigned to the first and third slots, respectively.

Based on the command of the mother PC, the mother communication device transmits the rotational speed command to device 1 at the beginning time of slot 1. Then, the blower responds to the PCU with the current rotational speed at the center time of slot 1. Similarly, in slot 3, the command of the rotational speed and response of the current rotational speed takes place between the PCU and device 2.

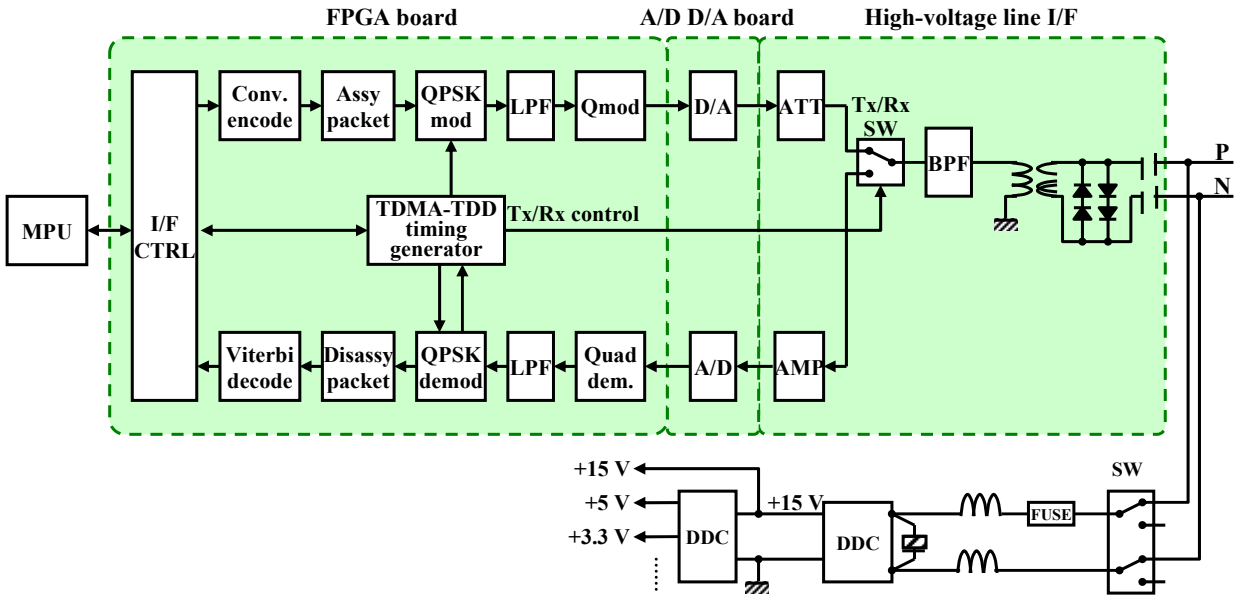

Fig. 10 A functional block diagram of the prototype of the communication device.

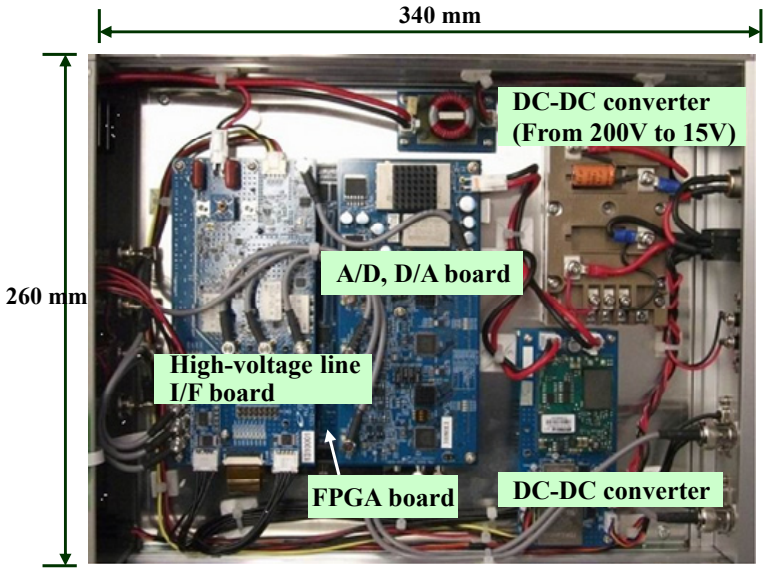

Fig. 11 A photo of the communication equipment.

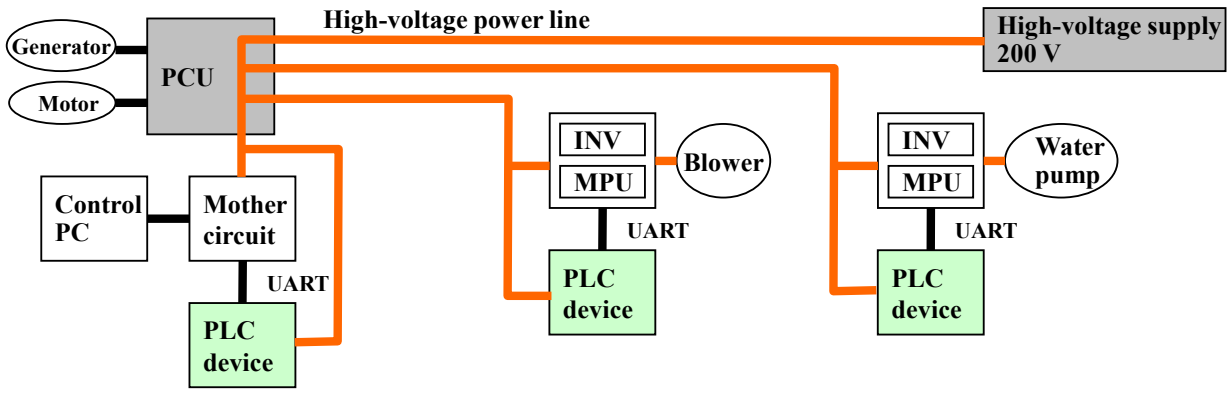

Fig. 12 A configuration of a high-voltage PLC system.

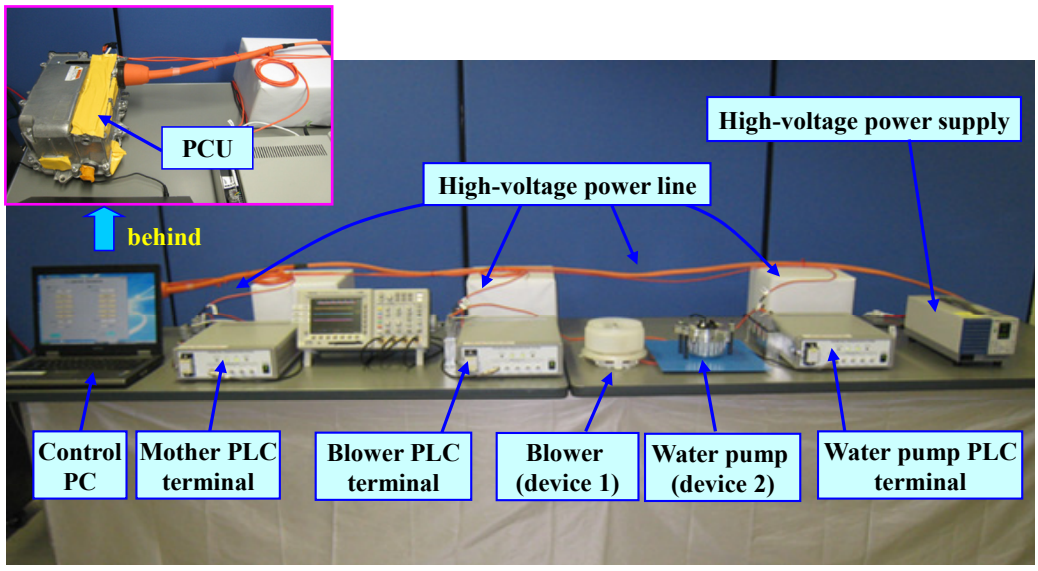

Fig. 13 A photo of the PLC system.

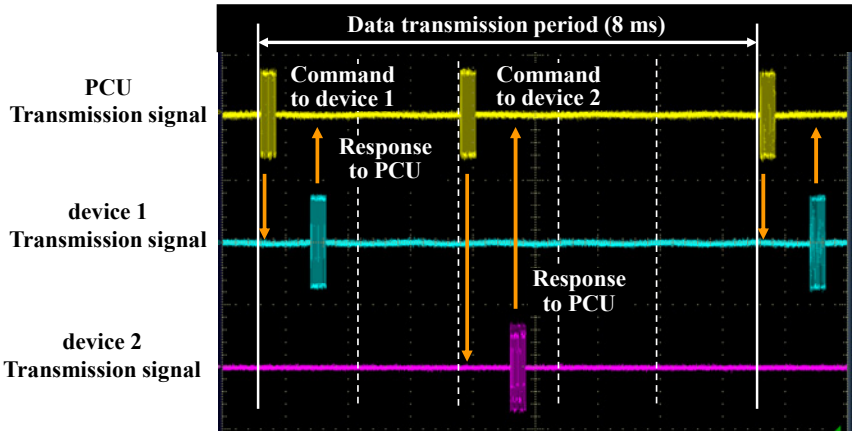

Fig. 14 An example of operation waveform of communication device.

In this system, the two motors are confirmed to respond correctly to the command even under the condition in which the rotational speeds of both the water pump and the blower are changed. From the above, we demonstrate the possibility of simultaneously controlling multiple power electronic devices in real time based on our proposed high-voltage PLC system.

8. Conclusions

Herein, we reported on the development of an HV high-voltage line PLC system that can simultaneously control multiple power electronic devices in real time. We began by evaluating vehicle power supply line transmission characteristics in order to determine the optimum carrier frequency in the PLC, and then clarified the noise characteristics overlaid on the line of a recent model HV. We then conducted computer simulations to evaluate the BER under the clarified noise environment. Next, we determined the system specifications of a dedicated communication device that will be used in the prototype of our proposed high-voltage line PLC system and demonstrated its ability simultaneously control the rotational speed of two motors.

In the future, it is anticipated that this technique will not only be used for PCU to electronic device communications, it is also expected to be adapted to internal high-voltage battery communications.

References

(1) Schiffer, A., “Statistical Channel and Noise Modeling of Vehicular DC Lines for Data Communication”, *Proc. IEEE Veh. Tec. Conf.*, Vol. 1 (2000), pp. 158-162.
(2) Carrion, M. O., Lienard, M. and Degauque, P., “Communication over Vehicular DC Lines: Propagation Channel Characteristics”, *Proc. IEEE Int. Symp. Power Line Commun. and Its Appl.*, Vol. 57, No. 2 (2006), pp. 2-5.
(3) Lenard, M., Carrion, M., Degardin, V. and Degauque, P., “Modeling and Analysis of In-vehicle Power Line Communication Channels”, *IEEE Trans. Veh. Tec.*, Vol. 57, No. 2 (2008), pp. 670-679.
(4) Vallejo-Mora, A., S´anchez-Mart´ınez, J., Ca˜nete, F., Cort´es, J. and D´ıez, L., “Characterization and Evaluation of In-vehicle Power Line Channels”, *Proc. IEEE Global Telecommun. Conf.* (2010), pp. 1-5.
(5) Bassi, E., Benzi, F., Almeida, F. and Nolte, T., “Powerline Communication in Electric Vehicles”, *Proc. IEEE Int. Electric Mach. Drives Conf.* (2009), pp. 1749-1753.
(6) Barmada, S., Raugi, M., Tucci, M. and Zheng, T., “Power Line Communication in a Full Electric Vehicle: Measurements, Modeling and Analysis”, *Proc. IEEE. Int. Symp. Power Line Commun. and Its Appl.* (2010), pp. 331-336.
(7) Taherinejad, N., Rosales, R., Lampe, L. and Mirabbasi, S., “Channel Characterization for Power Line Communication in a Hybrid Electric Vehicle”, *Proc. IEEE. Int. Symp. Power Line Commun. and Its Appl.* (2012), pp. 328-333.
(8) Nakano, Y., Umehara, D., Kawai, M. and Morihiro, Y., “Viterbi Decoding for Convolutional Code over Class A Noise Channel”, *Proc. IEEE. Int. Symp. Power Line Commun. and Its Appl.* (2003), pp. 97-102.

Masaki Takanashi

Research Fields:
- Communication System
- Security

Academic Degree: Ph.D.
Academic Societies:
- The Institute of Electronics, Information and Communication Engineers
- IEEE

Tomohisa Harada

Research Field:
- Digital Control System for Power Converter

Atsuhiro Takahashi
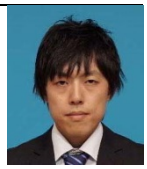
Research Fields:
- Electro-magnetic Compatibility (EMC) for Hybrid Vehicle
- Analysis of Electromagnetic Field Using FEM
- Topology Optimization

Academic Society:
- The Institute of Electronics, Information and Communication Engineers

Hiroya Tanaka

Research Field:
- Nanostructured Electromagnetic Devices

Academic Degree: Dr.Eng.
Academic Society:
- IEEE

Hiroaki Hayashi

Research Fields:
- EMC (Electromagnetic Compatibility) Design of IC
- Analog and RF IC Design

Academic Society:
- The Institute of Electronics, Information and Communication Engineers

Yoshiyuki Hattori

Research Fields:
- Electronic Devices for Automotive Application
- Electromagnetic Compatibility for Hybrid Vehicle

Academic Degree: Dr.Eng.
Academic Societies:
- The Institute of Electronics, Information and Communication Engineers
- The Institute of Electrical Engineers of Japan
- Society of Automotive Engineers of Japan

